

See discussions, stats, and author profiles for this publication at: <https://www.researchgate.net/publication/280880298>

Improved Imaging of Cleared Samples with ZEISS Lightsheet Z.1.: Refractive Index of Demand

Technical Report · July 2015

DOI: 10.13140/RG.2.1.1875.4408

CITATION

1

READS

968

4 authors, including:



Mattia Carraro

Science Meets Design Inc

8 PUBLICATIONS 63 CITATIONS

SEE PROFILE



Robert V Harrison

The Hospital for Sick Children, and University of Toronto

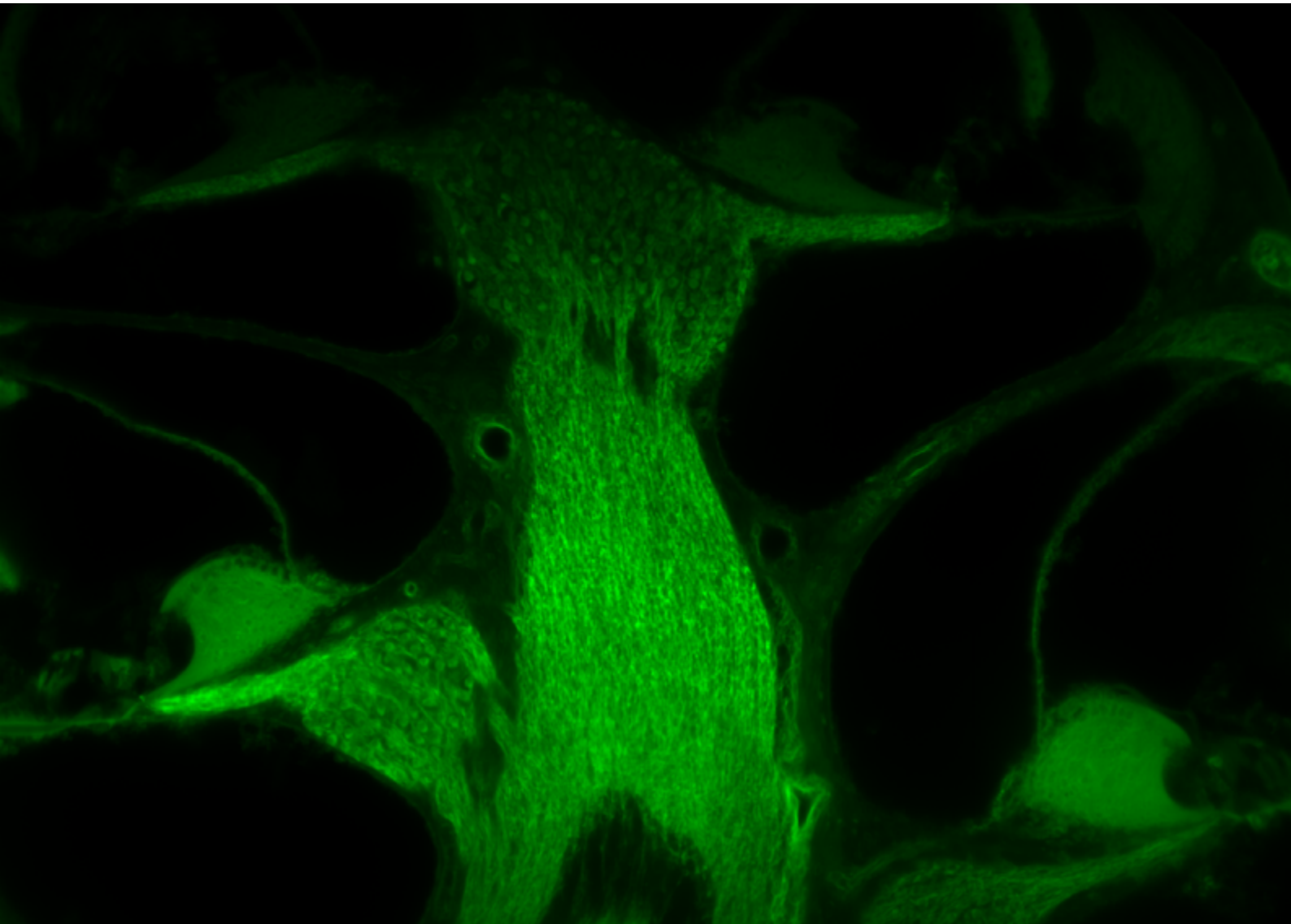
210 PUBLICATIONS 5,504 CITATIONS

SEE PROFILE

Some of the authors of this publication are also working on these related projects:



plasticity of tonotopic projections from cochlea to cortex [View project](#)



Improved Imaging of Cleared Samples with ZEISS Lightsheet Z.1:

Refractive Index on Demand



We make it visible.

Improved Imaging of Cleared Samples with ZEISS Lightsheet Z.1: Refractive Index on Demand

Author: Mattia Carraro^{1,2}, Paul Paroutis³, Michael Woodside³ and Robert V. Harrison^{1,2,4}
¹ *Auditory Science Laboratory, The Hospital for Sick Children, Toronto, ON, Canada.*
² *Institute of Biomaterials and Biomedical Engineering, University of Toronto, Toronto, ON, Canada.*
³ *Imaging Facility, The Hospital for Sick Children, Toronto, ON, Canada.*
⁴ *Department of Otolaryngology – Head and Neck Surgery, University of Toronto, Toronto, ON, Canada.*

Date: July 2015

Introduction

Light Sheet Fluorescence Microscopy (LSFM) uses a thin plane of light (light sheet) to optically section transparent tissues or whole organisms that have been fluorescently labeled. The emitted light is collected by a separate objective positioned perpendicular to the light sheet plane, allowing the imaging of the (excited) tissue during the illumination of only a single thin section of the sample. With no need for a pinhole aperture, the full optical section plane can be captured at once, providing a faster solution compared to laser scanning microscopes¹⁻⁷.

Compared to magnetic resonance imaging (MRI) and micro-computerized tomography (micro CT), both non-destructive imaging methodologies, the LSFM can achieve better spatial resolution (subcellular) and faster imaging speeds². In addition LSFM offers lower photo-bleaching and photo-toxicity, and the capability of imaging thicker tissues (>1 cm) compared to confocal or even two-photon microscopes². Furthermore, the LSFM microscope from ZEISS, Lightsheet Z.1, can rotate the sample 360°, enabling image acquisition with different angles of view (Multiview) from which a 3D image can be reconstructed. For example using appropriate software^{8,9} and mounting techniques¹⁰, images can be deconvolved and registered to obtain a single high-resolution 3D image file that can be viewed and interrogated with ZEN Imaging software or arivis Vision4D [arivis AG, Munich, Germany].

Light penetration in large samples (e.g., whole mouse brain tissue) is limited and requires removal of the opaque

components of the sample, a technique referred to as clearing. Several tissue clearing protocols have been developed, all of them focused on homogenizing the refractive index (RI) within the sample and some of them based on lipid removal¹¹⁻²³. Only one published method²¹ describes a variable RI, but the transparency achieved is limited and the minimum time needed to completely clear the specimen is 2 weeks. On the other hand, organic solvent based clearing approaches^{11,13,14,24,25} are straightforward and rapid²⁶, e.g. 3 to 5 days to produce very transparent specimens, but have some drawbacks. For example they result in decreased signals from GFP-like proteins, and are corrosive for most objectives; most importantly their RI cannot be easily adjusted. Typically these (corrosive) organic solvents have non-adjustable RIs between 1.53 – 1.56. Matching of the imaging solution to the sample RI and the imaging objective RI is important to avoid spherical aberration. Even small mismatches in RI can produce significant decreases in images resolution and brightness^{27,28}.

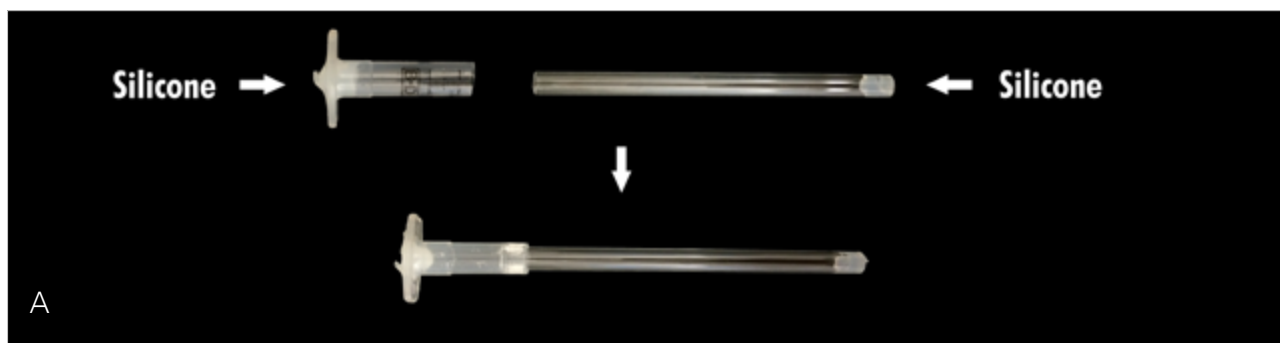


Figure 1 Illustration of the steps to seal the Simax tube that will contain the non-compatible chemicals. The cut barrel of 1 ml syringe is sealed with silicone as well as the Simax tube. Then, the sample cleared with ARIM is inserted in the tube and covered with fresh ARIM. Finally, both parts are mounted together.

ZEISS Lightsheet Z.1 is a state of the art LSFM that uses an immersion objective (Clr Plan- Neofluar 20x/1.0, $nd = 1.45 \pm 0.03$) to image cleared specimens⁶. Here we are presenting a solution to expand the range of compatible protocols for ZEISS Lightsheet Z.1. Although this particular approach has been developed specifically for ZEISS Lightsheet Z.1, similar approaches can be used in other LSFM that share similar limitations.

Our novel technical development is based on Lorentz-Lorenz equation²⁹ to formulate the optimum RI, combined with the use of a special chamber to contain the non-compatible solution without compromising image quality or damaging the LSFM system. We developed our “RI matching” solution based on the published 3DISCO, an organic-solvent based protocol, because it is rapid, reliable and does not require special equipment^{13,14,24,25}.

Methods

Use of non-compatible solutions

Since ZEISS Lightsheet Z.1 or the dipping objectives could be damaged by solvent fumes²⁶, it is necessary to image non-compatible solution specimens in a sealed container.

We found that Simax glass tubing [Kavalierglass A.S., Křižová, Czech Republic], a special borosilicate formulation, has a RI of n_{20}/D 1.472, it is resistant to the dibenzyl ether and, with custom-made adaptors, can be used as an imaging chamber

for ZEISS Lightsheet Z.1. As illustrated in Figure 1, one end of the Simax tube is sealed with silicone (water resistant, general purpose silicone) and after the curing is complete, the clearing solution and the sample can be inserted from the open end; it is important to avoid air bubbles. Finally, the tube is sealed with a custom-made adaptor for attachment to the imaging stage. The adaptor is made from a 1 ml syringe. The plunger is removed and the syringe is cut near the top (Figure 1) and the apical end of the barrel is sealed with silicone. The borosilicate tube and the adaptor are tightly sealed together. The specimen tube can be attached to the stage of ZEISS Lightsheet Z.1 with the syringe holder.

In the example of Figure 1, we used a Simax tube with an outer diameter of 5 mm and an inner diameter of 3.4 mm and cut 80 mm in length. Different diameter tubes can be used taking into account that the adaptor should be modified accordingly.

Refractive Index on Demand

After the tissue of interest is fixed and dissected, it has to be dehydrated and cleared. We follow the published methodology called 3DISCO^{13,14,24,25}. When the specimen is completely dehydrated, the RI has to be adjusted immersing the specimen in the Adjusted Refractive Index Medium (ARIM).

In the case of ZEISS Lightsheet Z.1, the Clarity objective has an adjustable RI correction collar (RI 1.42 to 1.48), which can be adjusted to match the Simax glass tubing (n_{20}/D 1.472) and the RI of the glycerol (n_{20}/D 1.472) solution

surrounding glass tubing. For optimum RI matching, the specimen RI should be matched to (n20/D 1.472).

To compute the correct liquid mixture that we would need to achieve the ARIM, the Lorentz-Lorenz equation can be used²⁹.

$$\text{Lorentz - Lorenz } (L - L): \frac{Z^2 - 1}{Z^2 + 2} = \frac{X^2 - 1}{X^2 + 2} \phi_1 + \frac{Y^2 - 1}{Y^2 + 2} \phi_2$$

$$\phi_i = \frac{c_i}{\rho_i}$$

$$Z = X\phi_1 + Y\phi_2$$

where

Z = RI of the desired mixture.

X = RI of the pure component 1.

Y = RI of the pure component 2.

c_i = concentration of the i th component (g/ml).

This is our unknown factor.

ρ_i = density of the i th component.

ϕ_i = volume fraction of the i th component.

$i = 1, 2 \dots n$.

Solving the set of simultaneous equations, we can formulate a clearing solution with the desired RI:

$$L - L: \frac{Z^2 - 1}{Z^2 + 2} = \frac{1.3616^2 - 1}{1.3616^2 + 2} * \frac{c_1}{0.789} + \frac{1.562^2 - 1}{1.562^2 + 2} * \frac{c_2}{1.02214}$$

$$Z = 1.3616 * \frac{c_1}{0.789} + 1.562 * \frac{c_2}{1.02214}$$

$$Z = 1.472$$

The result would be:

$$c_1 = 0.3304$$

$$c_2 = 0.59$$

Therefore, the volume fraction ϕ_i of each component would be c_i divided by ρ_i . In this particular case, the ethanol volume would be 0.418 ml and the DBE volume would be 0.578 ml.

Note that the sum of both components is not 1. That is because the volumes are non-additive.

The ARIM we created was a mixture of two compatible liquids, ethanol (RI of n20/D 1.3616) and dibenzyl ether (RI of n20/D 1.562), but it can be any mixture of liquids. The only limitation is that both solutions have to be compatible and soluble with each other, and that one of them has to have a RI superior than the one desired. It is also important to note that RI is related to light wavelength, so the stated RI of a solution should be accurate for the laser light wavelengths used on the scope.

Once the ARIM is prepared, the specimen from ethyl alcohol (or tetrahydrofuran) has to be immersed several times in it with increasing durations, e.g. 15 minutes, 30 minutes, 60 minutes (times have to be adjusted depending on the sample). All the steps are carried on a rotatory agitator, at room temperature, in a glass container of 7.5 ml, completely filled with solution and air tight sealed. Just before imaging, the solution should be changed again.

Results

Using this methodology we can theoretically have an almost negligible, 0.0002 RI mismatch between the glycerol and Simax glass, reducing image spherical aberration to almost zero. To have the best image possible, some trial and error may be required. For example, in certain samples it can be better to compromise the match in RI in order to achieve better transparency, as the mismatch can be somewhat corrected with the Multiview reconstruction and the computation of the point spread function^{8,9}.

In figure 2, we illustrate the improvement in resolution with the ARIM solution, compared to a non-adjusted RI.

The specimen here is the mouse inner ear (cochlea) specifically focused on the spiral ganglion cells and cochlear nerve bundles. Note that the image has not been reconstructed with any Multiview approximation.

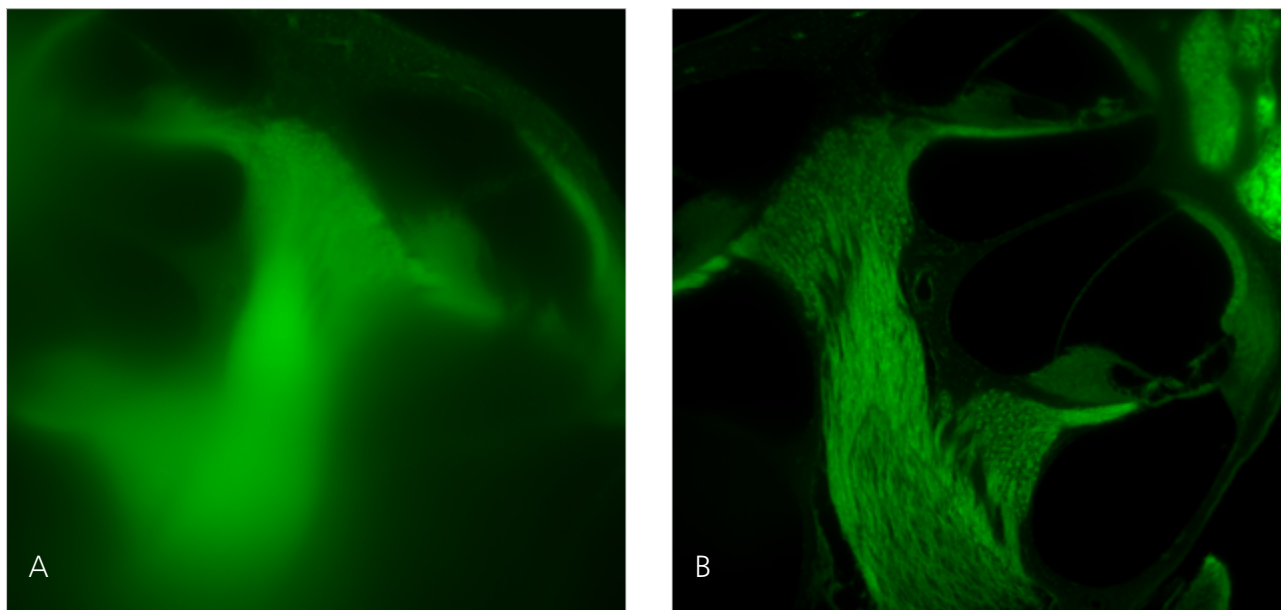


Figure 2 Comparison of a RI mismatch and match in the same specimen of a mouse cochlea. In [A] there is a RI mismatch of approx. 0.03. The image in [B] is achieved with a close RI match. Here the cell bodies and axonal elements are clearly resolved. The image has been captured from autofluorescence only and the depth is around 700 μm .

Discussion

The matching of RI between microscope objective, specimen holder and tissue medium is critical for light imaging of large specimens at depth. There is a large variety in protocols for tissue preparation, (e.g. clearing) each resulting in a specimen with a specific RI. Very few descriptions exist that allow optimal adjustment of RI. The aim of our investigation was

to expand on the number recommended clearing methods for ZEISS Lightsheet Z.1 without risking microscope damage or a significant compromise of image quality. However the approach described here can be expanded to any other scope for which similar problems exist. Moreover, the flexible approach described here can be useful when scope objectives (with different RIs) are changed or upgraded.

References:

- [1] Huisken, J., Swoger, J., Del Bene, F., Wittbrodt, J. & Stelzer, E. H. K. Optical Sectioning Deep Inside Live Embryos by Selective Plane Illumination Microscopy. *Science* (80-.). 305, (2004).
- [2] Santi, P. a. Light sheet fluorescence microscopy: a review. *J. Histochem. Cytochem.* 59, 129–38 (2011).
- [3] Santi, P. a et al. Thin-sheet laser imaging microscopy for optical sectioning of thick tissues. *Biotechniques* 46, 287–94 (2009).
- [4] Siedentopf, H. & Zsigmondy, R. Über Sichtbarmachung und Größenbestimmung ultramikroskopischer Teilchen, mit besonderer Anwendung auf Goldrubingläser. *Ann. Phys. (N. Y).* 315, (1902).
- [5] Yakimovich, A. A. & Andriasyan, V. Fast Imaging of Cellular Spheroids with Light Sheet Fluorescence Microscopy Fast Imaging of Cellular Spheroids with Light Sheet Fluorescence Microscopy.
- [6] Carl Zeiss Microscopy GmbH. ZEISS Lightsheet Z.1: Light Sheet Fluorescence Microscopy for Multiview Imaging of Large Specimens. (2014).
- [7] Voie, A. H., Burns, D. H. & Spelman, F. A. Orthogonal-plane fluorescence optical sectioning: three-dimensional imaging of macroscopic biological specimens. *J. Microsc.* 170, (1993).
- [8] Preibisch, S., Saalfeld, S., Schindelin, J. & Tomancak, P. Software for bead-based registration of selective plane illumination microscopy data. *Nat. Methods* 7, 418–419 (2010).

References:

- [9] Preibisch, S. et al. Efficient Bayesian-based multiview deconvolution. *Nat. Methods* 11, 645–8 (2014).
- [10] Carl Zeiss Microscopy GmbH. ZEISS Lightsheet Z.1: Sample Preparation. (2013). at http://microscopy.zeiss.com/microscopy/en_de/products/imaging-systems/lightsheet-z-1.html#Introduction
- [11] Becker, K., Jährling, N., Saghafi, S., Weiler, R. & Dodt, H.-U. Chemical clearing and dehydration of GFP expressing mouse brains. *PLoS One* 7, e33916 (2012).
- [12] Chung, K. & Deisseroth, K. CLARITY for mapping the nervous system. *Nat. Methods* 10, 508–13 (2013).
- [13] Ertürk, A. & Bradke, F. High-resolution imaging of entire organs by 3-dimensional imaging of solvent cleared organs (3DISCO). *Exp. Neurol.* 242, 57–64 (2013).
- [14] Ertürk, A., Lafkas, D. & Chalouni, C. Imaging Cleared Intact Biological Systems at a Cellular Level by 3DISCO. *J. Vis. Exp.* 1–13 (2014). doi:10.3791/51382
- [15] Ke, M.-T., Fujimoto, S. & Imai, T. SeeDB: a simple and morphology-preserving optical clearing agent for neuronal circuit reconstruction. *Nat. Neurosci.* 16, 1154–61 (2013).
- [16] Kuwajima, T. et al. ClearT: a detergent- and solvent-free clearing method for neuronal and non-neuronal tissue. *Development* 140, 1364–8 (2013).
- [17] Renier, N. et al. iDISCO: A Simple, Rapid Method to Immunolabel Large Tissue Samples for Volume Imaging. *Cell* 159, 896–910 (2014).
- [18] Susaki, E. et al. Whole-brain imaging with single-cell resolution using chemical cocktails and computational analysis. *Cell* 157, 726–39 (2014).
- [19] Tainaka, K. et al. Whole-Body Imaging with Single-Cell Resolution by Tissue Decolorization. *Cell* 159, 911–924 (2014).
- [20] Tomer, R., Ye, L., Hsueh, B. & Deisseroth, K. Advanced CLARITY for rapid and high-resolution imaging of intact tissues. *Nat. Protoc.* 9, 1682–97 (2014).
- [21] Yang, B. et al. Single-Cell Phenotyping within Transparent Intact Tissue through Whole-Body Clearing. *Cell* 158, 945–958 (2014).
- [22] Yokomizo, T. et al. Whole-mount three-dimensional imaging of internally localized immunostained cells within mouse embryos. *Nat. Protoc.* 7, 421–31 (2012).
- [23] Marx, V. Microscopy: seeing through tissue. *Nat. Methods* 11, 1209–1214 (2014).
- [24] Ertürk, A. et al. Three-dimensional imaging of solvent-cleared organs using 3DISCO. *Nat. Protoc.* 7, 1983–1995 (2012).
- [25] Ertürk, A. et al. Three-dimensional imaging of the unsectioned adult spinal cord to assess axon regeneration and glial responses after injury. *Nat. Med.* 18, 166–171 (2011).
- [26] Carl Zeiss Microscopy GmbH. ZEISS Lightsheet Z.1 Clearing Options. (2014).
- [27] Egnér, A. & Hell, S. W. Aberrations in confocal and multi-photon fluorescence microscopy induced by refractive index mismatch. *Handb. Biol. Confocal Microsc.* Third Ed. 404–413 (2006). doi:10.1007/978-0-387-45524-2_20
- [28] Diaspro, A., Federici, F. & Robello, M. Influence of refractive-index mismatch in high-resolution three-dimensional confocal microscopy. *Appl. Opt.* 41, 685–690 (2002).
- [29] Heller, W. Remarks on Refractive Index Mixture Rules. *J. Phys. Chem.* 69, 1123–1129 (1966).



Carl Zeiss Microscopy GmbH
07745 Jena, Germany
microscopy@zeiss.com
www.zeiss.com/microscopy



We make it visible.